# Effect of IBDV infection on the interfollicular epithelium of chicken bursa of Fabricius

Ildikó Bódi,[*] Balázs Felföldi,[‡] Krisztina Minkó,[*] Zsófia Benyeda,[†] Nándor Nagy,[*] Anna L Kiss,[*] Vilmos Palya,[‡] and Imre Oláh[*,1]

[*]*Department of Anatomy, Histology and Embryology, Semmelweis University, Budapest 1094, Hungary;* [†]*Biovo Animal Health Ltd., 7700 Mohács, Hungary; and* [‡]*Ceva-Phylaxia Ltd., 1107 Budapest, Hungary*

**ABSTRACT** In the chicken bursa of Fabricius (**BF**), the interfollicular epithelium (**IFE**) consists of cylindrical- and cuboidal-shaped cells. Among the cylindrical-shaped epithelial cells, mucus-producing and caveolin-1 (**Cav-1**)-expressing cells can be distinguished. Occasionally, the cuboidal-shaped cells also express Cav-1, which suggests that they are precursors of both mucus-producing and Cav-1-expressing cells. Very virulent infectious bursal disease virus (**IBDV**) impedes the differentiation of Cav-1-expressing cells and shifts the differentiation of cuboidal cells towards mucus-producing cells. In control birds exclusively, the IFE surface shows a mucous membrane, but after IBDV infection, the surfaces of both IFE and FAE are also covered by a mucous membrane. After IBDV infection, the cells of FAE also produce mucus, providing evidence for cell transformation. In late postinfection (**pi**; 28 d pi), the Cav-1 expression returned in the IFE cells, whereas the follicle (the primary lymphoid organ) underwent atrophy. The appearance of the renewed Cav-1-positive cells is similar to that of the normal basal cell, but they randomly locate in different levels of IFE, suggesting the loss of epithelial polarity. Between days 2 and 7 pi, the Cav-1 expression in the endothelial cells of the cortico-medullary capillary web is variable, which may explain the hemorrhage in several infected birds. The IBDV infection stops the Cav-1 expression and subsequently the cholesterol efflux into the bursal lumen. In the infected birds, the high cholesterol level may further worsen the clinical syndrome of IBDV.

**Key words:** interfollicular epithelium, caveolin-1, mucous membrane, IBDV infection, transformation of FAE and medullary reticular epithelial cell

2019 Poultry Science 98:3464–3470
http://dx.doi.org/10.3382/ps/pey512

## INTRODUCTION

Bursa of Fabricius (**BF**) is a complex organ. (i) The follicle with the follicle-associated epithelium (**FAE**) is a primary lymphoid tissue, which is responsible for B-cell maturation and survival. (ii) A considerable number of interfollicular epithelial cells (**IFE**) express caveolin-1 (**Cav-1**) and contribute to cholesterol homeostasis by cholesterol efflux into the bursal lumen (Bódi et al., 2017). (iii) The endothelial cells of the cortico-medullary (**CM**) capillary web also express Cav-1, which influences the bursal growth (Farsang et al., 2018).

Cav-1 is an integral membrane protein, localized in the plasma membrane invaginations (caveolae), trans-Golgi-network (**TGN**), and vesicular structures of the cytoplasm (Rothberg et al., 1992; Couet et al., 2001; Razani and Lisanti, 2002; Goetz et al., 2008). It is involved in numerous cellular and physiological functions (Parton and Simons, 2007; Feng et al., 2013): intracellular cholesterol transport, cholesterol homeostasis and cholesterol efflux (Fielding and Fielding, 1995, 1997, 2001; van Deurs et al., 2003; Martin and Parton, 2005; Frank et al., 2006), endocytosis (Pelkmans and Helenius, 2002; PU et al., 2002; Kiss, 2012), cell migration (Navarro et al., 2004), and cell differentiation (Ravid et al., 2006; Parton and Simons, 2007; Björnstad et al., 2014; Guan et al., 2016). A large number of caveolae can be found in endothelial cells (van Deurs et al., 2003; Navarro et al., 2004), adipocytes (Razani et al., 2002; Guan et al., 2016), fibroblasts (Razani et al., 2002), and type I pneumocytes (Jung et al., 2012; Björnstad et al., 2014). Cav-1 can mediate simian virus 40 uptake through caveolae, and the internalized caveolae carry the virus into smooth-surfaced endoplasmic reticulum (Pelkmans et al., 2001).

Vascular system is a dynamic organ, which is able to react and adapt rapidly to internal and external demands. Capillaries are important vessels; hence, most of the exchange of water, water-soluble substances, and respiratory gases takes place through the capillary wall. Transcytosis in the endothelial cells (van Deurs et al., 2003; Navarro et al., 2004) is one of the fundamental


Received August 2, 2018.
Accepted October 29, 2018.
[1]**Corresponding author:** olah.imre@med.semmelweis-univ.hu

processes by which the endothelial cells contribute to the communication between blood and tissues. The endothelial transcytosis is a basic cytological function that is carried out by caveolae. Cav-1 binds cholesterol in 1 to 1 ratio; therefore, the changes in the Cav-1 expression influence the cholesterol homeostasis. The excess free cholesterol is toxic (Warner et al., 1995; Fielding and Fielding, 1997); therefore, the cholesterol efflux from the IFE could be essential for the bird. The middle plical vessel (**MPV**) of BF branches off to form interfollicular arterioles, from which the CM capillary web offshoots (Schoenwolf et al., 1981; Abbate et al., 2007) for supplying the follicular cortex and medulla. Serious infection of infectious bursa disease virus (**IBDV**) may result in hemorrhage in the BF, and the CM capillary web is possibly the major site of bursal hemorrhage.

The aim of this study was to determine how the IBDV infection influences the Cav-1 expression and mucus-producing cells of the IFE and endothelial cells of the CM capillary web.

## MATERIALS AND METHODS

### Animals

Three-week-old White Leghorn layer type chickens (sex: mixed) of SPF status (Charles River) were used in the test. The chickens were reared under standard conditions on deep litter; feed (sterilized broiler grower mix) and water (tap water) were available ad libitum. The study was conducted in compliance with the provisions of Directive 2010/63/EU, Hungarian Act No. XXVIII/1998, and the Hungarian Governmental Decree No. PE/EA/151-4/2018 (I.29.) and with the permission of the Hungarian competent authority.

### Infection

IDBV infection was carried out using a very virulent field isolate (D407/02/04/TR). The virus suspension was diluted in steril phoshate buffer (**PBS**) and at a dose of 3.0 IgEID50/chicken in 0,2 ml PBS was applied orally. Tissue samples were collected 36 h, 2, 4, 7, 14, 21, and 28 d postinfection (**pi**). The chickens were humanly euthanized by $CO_2$ inhalation.

### Antibodies

Anti-IBDV monoclonal antibody 5A10 was received from Ceva-Phylaxia Ltd. (Budapest, Hungary). The antibody was produced against VP2 protein of IBDV. Polyclonal rabbit anti-Cav-1 was obtained from BD Transduction Laboratories (610406, BD Biosciences, San Jose, CA).

### Immunocytochemistry

Tissue samples were embedded in liver and frozen in liquid nitrogen. The 10 $\mu$m cryostat sections were fixed in cold acetone for 10 min and immunostained, as discussed (Bódi et al., 2017). Briefly, the sections were incubated with primary antibodies for 45 min, followed by an isotype-specific biotinylated secondary antibody. The binding sites of primary antibodies were detected by 4-chloro-naphtol (C8890, Sigma-Aldrich, Budapest, Hungary).

### Pre-embedding Immunohistochemistry for Transmission Electron Microscopy

Tissue samples were fixed in 4% paraformaldehyde for 60 min. After fixation, the tissue was washed 3 times in PBS and embedded in 7.5% gelatin. Fifty-micrometer-thick gelatin-embedded sections were cut with cryomicrotome and collected in PBS under a free-floating condition. For blocking the endogenous peroxidase, the sections were treated by 3% $H_2O_2$ (H1009, Sigma-Aldrich, Budapest, Hungary) for 30 min. After 30-min washing, anti Cav–1 antiserum diluted in PBS (1:200) containing 1% bovine serum–albumin was used for 2 h followed by the use of the avidin-biotin complex (1:100; Vectastain Elite PK–6100, Vector 115 Laboratories, Burlingame, CA) and biotin-conjugated goat anti–rabbit secondary antibody (1:200; BA–1100, Burlingame, CA) for 2 h. The immunoperoxidase reaction was developed with 3,3-diaminobenzidine (**DAB**; D8001, Sigma-Aldrich, Budapest, Hungary). After immunohistochemistry, the sections were post-fixed in 1% osmium tetroxide (23310-10, Polysciences Inc., Warrington, PA) for 10 min to preserve DAB staining. After dehydration in graded ethanol, the tissue sections were embedded in Polybed/Araldite 6500 (00552, Polysciences Inc. Warrington, PA) mixture and polymerized for 48 h at 60°C. The ultrathin sections were contrasted with uranyl acetate and lead citrate and studied with a Hitachi electron microscope, type H-7600.

Five-micron-thick paraffin sections were stained with rutin Hematoxylin–eosin staining and modified Movat pentachrome staining (Bancroft and Gamble 2002).

### Image Processing

Images were processed using Adobe Photoshop.

## RESULTS AND DISCUSSION

The IFE of the BF is a pseudostratified epithelium, which consists of cuboidal-shaped basal cells and cylindrical-shaped cells. Among the cylindrical-shaped cells, mucus-secreting (Figure 2a) and Cav-1-positive cells can be distinguished (Figure 1a). The Movat pentachrome staining shows the mucus in the apical

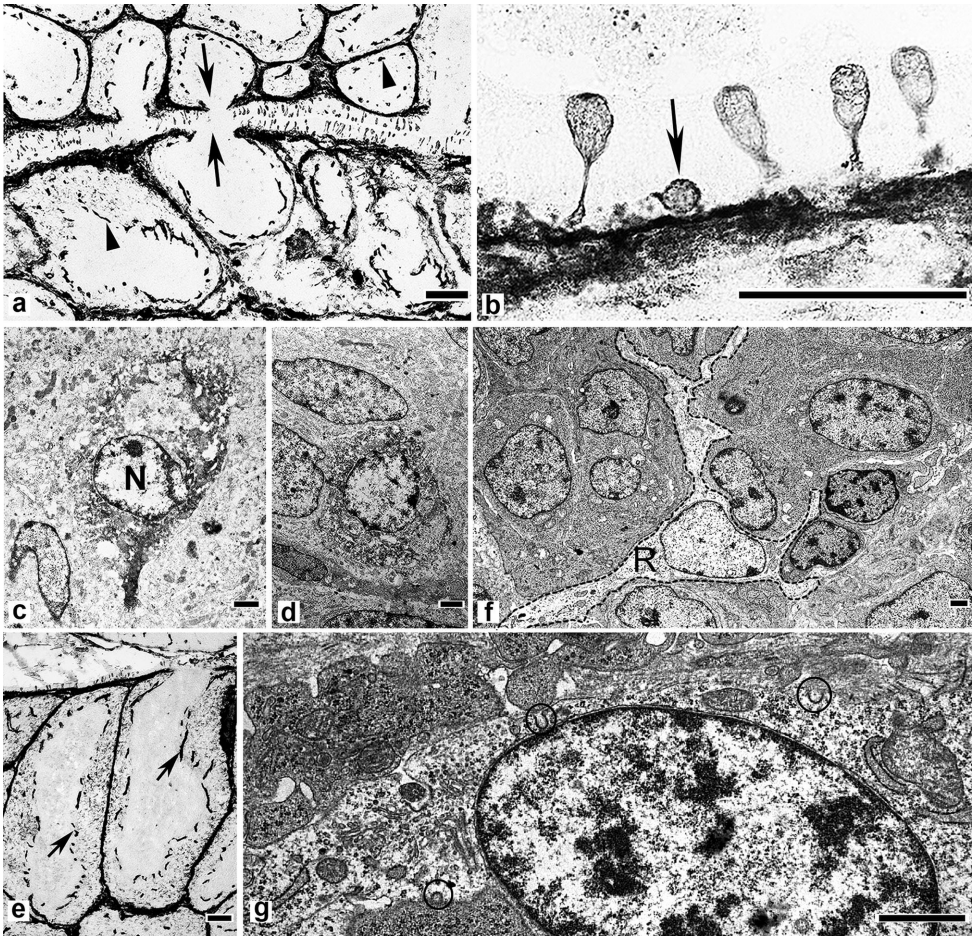


**Figure 1.** (a) Three-week-old control bird: Cav-1 immunostaining. In the IFE, numerous cells express Cav-1, but the FAE is Cav-1 negative (arrow). Fibrocytes and endothelial cells are heavily stained in the subepithelial and interfollicular connectives. In the endothelial cells of the CM capillary web, the Cav-1 expression is strong and clearly demarcates the follicular medulla (arrowhead). (b) The Cav-1-positive IFE cells are of the shape of a tennis racket. One of the basal cells also expresses Cav-1 (arrow). (c) The transmission electron microscopic immunocytochemistry confirms the shape of Cav-1-positive IFE cells. Surprisingly, the TGN area above the nucleus (N) seems to be free from the reaction product. (d) The transmission micrograph shows a Cav-1-positive basal cell. The immunocytochemical product surrounds the nucleus. (e) Cav-1 is expressed in the endothelial cells of the capillary web (arrows). Between the capillary web and interfollicular connective tissue (ct)—in the follicular cortex (C)—a fine Cav-1 network is formed. The follicular medulla (M) is devoid of Cav-1. (f) Cortical reticular cells (R) are stellate shaped (outlined). (g) The transmission micrograph shows coated vesicle-formation in a cortical reticular cell (circle). Bar: a and e: 100 $\mu$m, b: 50 $\mu$m, c and d, f and g: 1 $\mu$m.

portion of the IFE cells and the continuous mucous membrane on the surface epithelium of the IFE (Figure 2a). The cells of the FAE do not express Cav-1 (Figure 1a), and the mucous membrane is absent in the FAE (Figure 2a). In the FAE, the absence of Cav-1 suggests the lack of Cav-1-mediated endocytosis by the cells. The shape of the Cav-1-positive cell looks like a "tennis-racket" (Figure 1b). The "handle" of the racket starts close to the basal lamina, and below the nucleus, the "handle" splits and surrounds the nucleus and possibly the TGN above the nucleus (Figure 1c). The cytoplasm reveals a fine granulated reaction product (Figure 1b). Occasionally, the basal cell also expresses Cav-1 (Figure 1b and d). The Cav-1 appearance in the cuboidal-shaped basal cells suggests that these cells could be the precursor of both types of cylindrical-shaped cells; for example, they function as "epithelial progenitor or stem cells," although mitosis in these cells cannot be found; however, their number decreases with age, and in late IBDV infection (Figure 2g).

The follicular cortex expresses a very fine Cav-1-positive network (Figure 1f), which may be related to the cortical reticular cells (Figure 1e and g). The transmission micrograph shows coated vesicle-formation in the reticular cell's membrane (Figure 1g).

The effect of Gumboro virus infection on the primary lymphoid organ of the BF is well-documented, both morphologically (Käufer and Weiss, 1976; Panisup et al., 1988; Ramm et al., 1991; Vervelde and Davison, 1997) and immunologically (Naqi et al., 1983; Rautenschlein et al., 2007; Ingrao et al., 2013). However, no information was available about the effect of viral infection on the cells of IFE. After 2 d pi, the $\alpha$-Gumboro immunostaining shows high variability among the bursal follicles (Figure 2d). A considerable number of follicles do not show $\alpha$-Gumboro staining, while in the

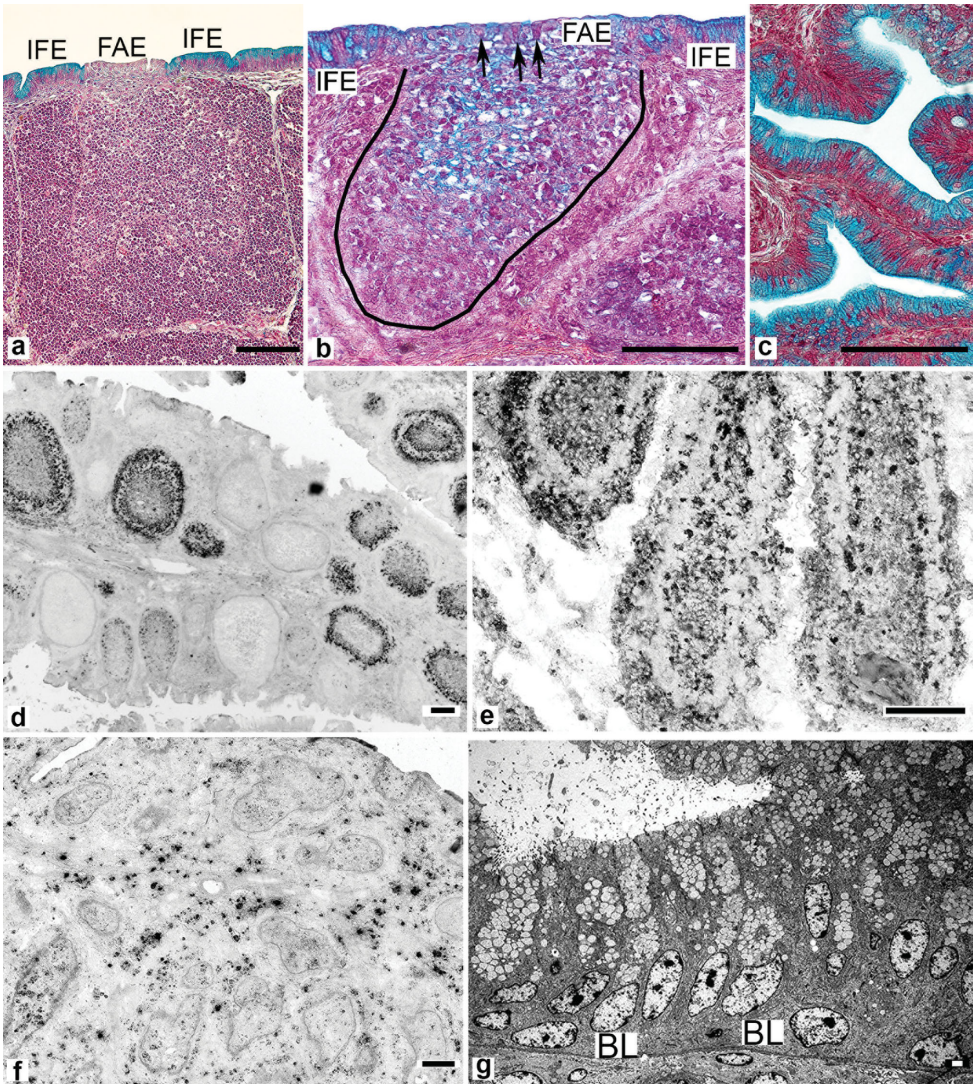


**Figure 2.** (a) Five-week-old control bird: Movat pentachrome staining. Secretory product and mucous membrane are in the apical portions of the cells on the surface of IFE (blue). Mucous membrane above the FAE is lacking. (b) Twenty-one days pi. Movat pentachrome staining. On the surface of the FAE, the mucus membrane appeared. In the FAE and follicular medulla, a secretory substance similar to that of IFE product emerged. The CM border is outlined. (c) Twenty-eight days pi. Movat pentachrome staining. The surface epithelium of the bursal fold is highly folded and the epithelial cells are Alcian blue. (d) Two days pi. The $\alpha$-Gumboro-stained section shows highly variable follicles. Besides the Gumboro-negative follicles, the Gumboro-positive cells form single and double rings. Scattered positive cells were found between the two rings. (e) Four days pi. The $\alpha$-Gumboro-positive cells of the inner ring are partially scattered over the follicular medulla, and the external ring locates at the marginal part of the follicular cortex. (f) Seven days pi. The medulla and cortex of the follicles almost cleared up from $\alpha$-Gumboro-positive cells. The Gumboro-positive cells occupy the interfollicular and axial connective tissues of the fold. (g) Fourteen days pi. The transmission micrograph shows that all cylindrical-shaped cells are packed with secretory granules. The number of basal cells (BL) decreased and a large gap appears between the cells. Bar: a, b, d, and f: 100 $\mu$m, c: 20 $\mu$m, and g: 1 $\mu$m.

positive follicles, the infected cells are localized in one or two rings. In the case of one ring, the $\alpha$-Gumboro-positive cells are located in the follicular medulla, close to the CM border. If there are two $\alpha$-Gumboro-positive rings, the outer ring is in the cortex, also close to the CM border (Figure 2d). Between the two $\alpha$-Gumboro-positive rings, there are scattered positive cells, which migrate between the cortex and medulla (Figure 2d). In this stage of pi, there is no significant alternation in the Cav-1-positive IFE cells. Between 2 and 7 d pi, the Cav-1 expression is variable in the endothelial cells of the CM capillary web, but the number of Cav-1-positive IFE cells drastically decreased by day 4 pi (Figure 3a). The variability in the histopathological signs of follicular infection does not reflect in the Cav-1 expression of the IFE cells, which suggests that the Cav-1 expression is independent of the primary lymphoid organ (FAE+follicle). The virus infection might have hindered the differentiating capacity of basal cells into Cav-1-positive cells. The differentiation is possibly shifted towards the mucus-secreting cell because in later stages of the infection, the surface epithelium is highly folded and consists of mucus-secreting cells (Figure 2c).

In control birds, the mucous membrane—as one of the subjects of innate immunity—covers the surface of the IFE, but not of the FAE (Figure 2a). The FAE

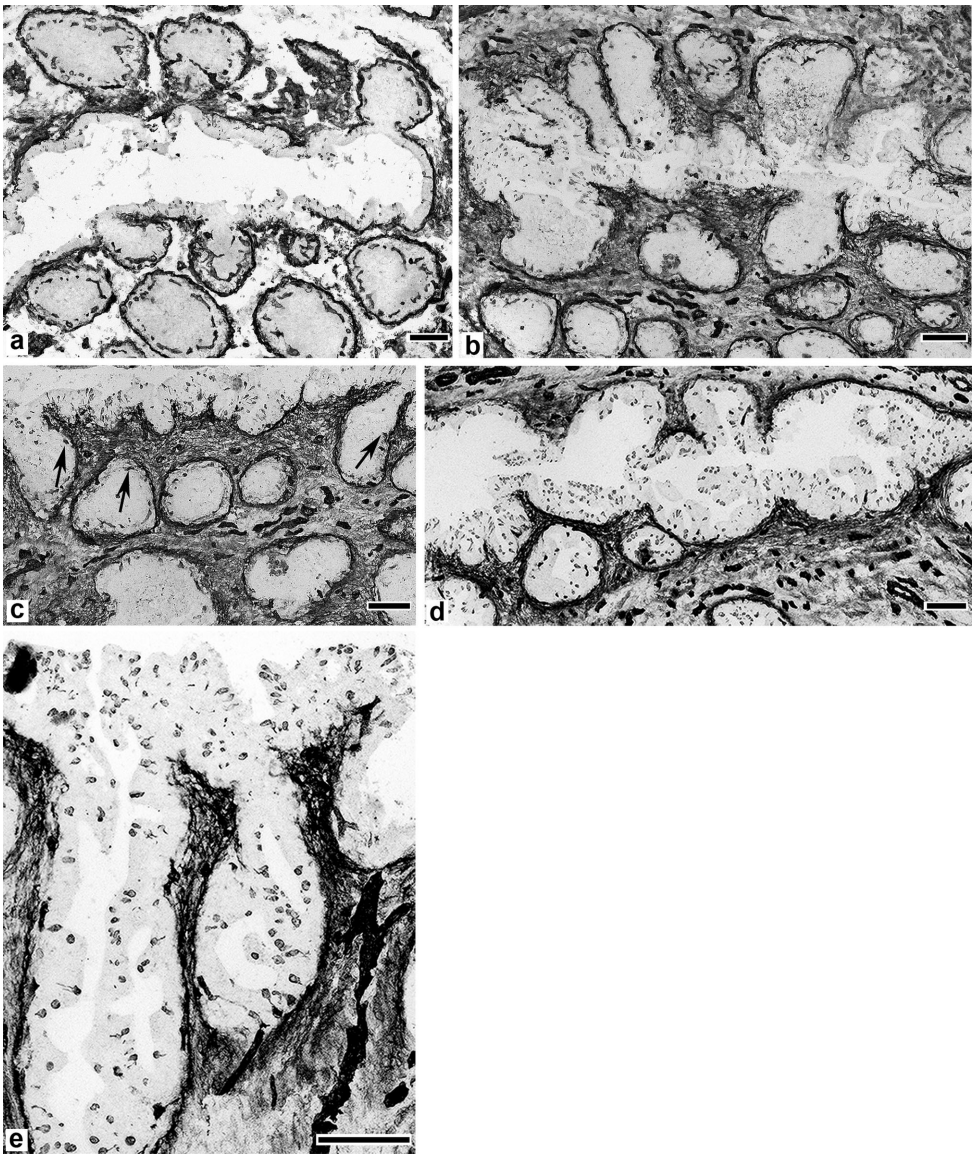


**Figure 3.** (a) Four days pi. Few Cav-1-positive IFE cells show only the "head" of tennis racket. The CM capillary web seems to be in a good condition. (b) Seven days pi. The appearance of Cav-1-positive IFE cells is similar to that of the cells by day 4 pi. But the density of the capillary web decreased. (c) Twenty-one days pi. The number of Cav-1-positive IFE cells is increased, but the capillary web is highly defective. Few portions of capillary web still persist (arrow). (d) Twenty-eight days pi. The follicular organization cannot be recognized, and the number of Cav-1-positive IFE cells definitely increased. (e) Higher magnification of the IFE. The shape of Cav-1-positive cells resembles the shape of normal Cav-1-expressing basal cells, but their position is irregular in the epithelium. Bar: 100 $\mu$m.

constructs 10% of the bursal surface. The number of FAE is 8,000 to 12,000/bursa, which appear as small islands in the IFE (Oláh and Glick, 1978). A question has been raised: How does the FAE exclude the mucous membrane? Is it possible that the viscosity of a mucous membrane is so high, "sticky" that it prevents its spreading on the bursal surface? Or the cells of FAE have a peculiar capacity to keep away the mucous substance?

After IBDV infection, the cells of FAE may have undergone transformation to be mucus-producing cells, and the mucous membrane appears on the surface of the transformed cells (Figure 2b). The "sticky" state of the mucous membrane may be supported by the finding that the mucous-negative FAE cells are devoid of a mucous membrane (Figure 2b). At this stage of infection, the FAE consists of two kinds of cells: (i) the sui generis FAE cells and (ii) mucus-producing transformed cells. The first one is devoid of a mucous membrane, and the second one reveals a mucous membrane. After IBDV infection, the regeneration capacity of bursal follicles may be influenced by the proportion of the two kinds of cells.

The mucous substance appears in the follicular medulla, but not in the follicular cortex, which may be produced by medullary epithelial reticular cells, or the cells of the FAE released the mucous substance into the intercellular space of medulla? Future studies should provide an answer to numerous questions, which touch the innate immunity of BF.

By day 4 pi, the α-Gumboro-positive cells of the inner ring are scattered over the medulla (Figure 2e). The interfollicular connective tissue does not show α-Gumboro-positive cells. There is a significant decrease in the number of Cav-1-positive IFE cells, and the majority of cells show only the "head" of tennis racket (Figure 3a). The Cav-1-positive IFE cell releases cholesterol into the bursal lumen (Bódi et al., 2017). The decreased number of Cav-1-positive cells suggests that the cholesterol efflux is also diminished or ceased. High cholesterol level is toxic for the bird, which may worsen the clinical syndrome of IBDV. The IBDV infection temporary stopped the differentiation of new Cav-1-positive cells. The drastic decrease in the number of Cav-1-positive cells took place by 4 d pi, which may allow us to estimate the differentiation time of Cav-1 and possibly also the mucin-secreting cells from the basal cells. The 4 to 5 d of differentiation time may be confirmed by the finding that a considerable number of Cav-1-positive cells emerged between 21 and 28 d pi. At day 7 pi, in the majority of follicles, the medulla and cortex were cleared from Gumboro-positive cells, but many virus-containing cells appeared in the interfollicular connective tissue (Figure 2f). In the IFE cells, Cav-1 expression can be seen only occasionally (Figure 3b). Parallel with the drastically decreased Cav-1-positive IFE cells, the number of the secretory cells increased, and almost every cylindrical-shaped cell is mucous positive (Figure 2g). In some places, the capillary web seems to be defective (not complete around the follicular medulla; Figure 3b). Possibly, the endothelial cells lost their capability for caveola formation. The absence of caveola formation in the endothelial cell of the capillary web results in the disappearance of transcytosis, which subsequently damages the communication between blood and bursal follicles. This phenomenon may result in bursal hemorrhage. At 21 d pi, Cav-1 expression may be found in few IFE cells and in the rest of the CM capillary web (Figure 3c). By day 28 pi, the follicular organization cannot be recognized, but many IFE cells again produced Cav-1 (Figure 3d and e). The shape of these Cav-1-positive cells looks similar to that of normal basal cells, and they appeared in different levels of the epithelium. By day 28 pi, these randomly localized Cav-1-positive cells in the IFE suggest that the IFE lost its polarity, which may be maintained by the primary lymphoid organ (FAE+follicle). This observation shows that Cav-1 expression is not re-established in the former Cav-1-positive cells, but the differentiation capability of basal cells might have been regained following the infection. In the MPV, the Cav-1 expression became strong, but the CM capillary web disappeared (Figure 3d).

## CONCLUSIONS

The atrophy of lymphoid tissues of BF and the return of Cav-1 expression in the IFE cells support the hypothesis that the BF is a complex organ (Bódi et al., 2017). The IFE consists of histologically and functionally three types of cells, and the differentiation and function of these cells are influenced by IBDV infection. (i) Mucus-secreting cells produce a mucous membrane that contributes to the innate immunity. After IBDV infection, the innate immunity overlaps the atrophying primary lymphoid organ. (ii) Cav-1-expressing cells contribute to cholesterol homeostasis of the bird by cholesterol efflux. Cholesterol efflux is ceased by IBDV infection. (iii) Basal cell, which serves as an epithelial progenitor cell, and the IBDV infection shift the differentiation towards mucous-producing cells.

## REFERENCES


Abbate, F., C. Pfarrer, C. J. Jones, E. Ciriaco, G. Germanà, and R. Leiser. 2007. Age-dependent changes in the pigeon bursa of Fabricius vasculature: a comparative study using light microscopy and scanning electron microscopy of vessel casts. J. Anat. 211:387–398.

Bancroft, J. D., and M. Gamble. 2002. Theory and practice of histological techniques. Pages 160–161, in Connective Tissues and Stains. J. D Bancroft, and M. Gamble ed., 5th ed. Churchill Livingstone, London, United Kingdom.

Björnstad, S., R. E. Paulsen, A. Erichsen, J. C. Glover, and B. Roald. 2014. Type I and II pneumocyte differentiation in the developing fetal chicken lung: conservation of pivotal proteins from birds to human in the struggle for life at birth. Neonatology 105:112–120.

Bódi, I., K. Minkó, O. Fölker, Z. Benyeda, B. Felföldi, A. Magyar, A. Kiss, V. Palya, and I. Oláh. 2018. Expression of caveolin-1 in the interfollicular but not the follicle-associated epithelial cells in the bursa of fabricius of chickens. J. Morphol. 279:17–26.

Couet, J., M. M. Belanger, E. Roussel, and M. C. Drolet. 2001. Cell biology of caveolae and caveolin. Adv. Drug. Deliv. Rev. 49:223–235.

Farsang, A., I. Bódi, O. Fölker, K. Minkó, Z. Benyeda, Á. Bálint, and I. Oláh. 2018. Coronavirus infection retards the development of the cortico-medullary capillary network in the bursa of Fabricius of chicken. Acta Vet. Hung. 66:20–27.

Feng, H., W. Guo, J. Han, and X. A. Li. 2013. Role of caveolin-1 and caveolae signaling in endotoxemia and sepsis. Life Sci. 93:1–6.

Fielding, P. E., and C. J. Fielding. 1995. Plasma membrane caveolae mediate the efflux of cellular free cholesterol. Biochemistry 34:14288–14292.

Fielding, C. J., and P. E. Fielding. 1997. Intracellular cholesterol transport. J. Lipid Res. 38:1503–1521.

Fielding, C. J., and P. E. Fielding. 2001. Caveolae and intracellular trafficking of cholesterol. Adv. Drug. Deliv. Rev. 49:251–264.

Frank, P. G., M. W. Cheung, S. Pavlides, G. Llaverias, D. S. Park, and M. P. Lisanti. 2006. Caveolin-1 and regulation of cellular cholesterol homeostasis. Am. J. Physiol. Heart Circ. Physiol. 291:H677–H686.

Goetz, J. G., P. Lajoie, S. M. Wiseman, and I. R. Nabi. 2008. Caveolin-1 in tumor progression: the good, the bad and the ugly. Cancer Metastasis Rev. 27:715–735.

Guan, X., N. Wang, F. Cui, Y. Liu Y, P. Liu P, J. Zhao, C. Han, X. Li, Z. Leng, Y. Li, X. Ji, W. Zou, and J. Liu. 2016. Caveolin-1 is essential in the differentiation of human adipose-derived stem cells into hepatocyte-like cells via an MAPK pathway-dependent mechanism. Mol. Med. Rep. 13:1487–1494.

Ingrao, F., F. Rauw, B. Lambrecht, and T. van den Berg. 2013. Infectious bursal disease: a complex host–pathogen interaction. Dev. Comp. Immunol. 41:429–438.

Jung, K., H. Schlenz, G. Krasteva, and C. Mühlfeld. 2012. Alveolar epithelial type II cells and their microenvironment in the caveolin-1-deficient mouse. Anat. Rec. 295:196–200.

Käufer, I., and E. Weiss. 1976. Electron-microscope studies on the pathogenesis of infectious bursal disease after

intrabursal application of the causal virus. Avian Dis. 20:483–495.
Kiss, A. L. 2012. Caveolae and the regulation of endocytosis. Adv. Exp. Med. Biol. 729:14–28.
Martin, S., and R. G. Parton. 2005. Caveolin, cholesterol, and lipid bodies. Sem. Cell Dev. Biol. 16:163–174.
Naqi, S. A., B. Marquez, and N. Sahin. 1983. Maternal antibody and its effect on infectious bursal disease immunization. Avian Dis. 27:623–631.
Navarro, A., B. Anand-Apte, and M. O. Parat. 2004. A role for caveolae in cell migration. FASEB J. 18:1801–1811.
Oláh, I., and R. Glick. 1978. The number and size of the follicular epithelium (FE) and follicles in the bursa of fabricius. Poult. Sci. 57:1445–1450
Panisup, A. S., B. Järplid, K. C. Verma, and G. C. Mohanty. 1988. Electron microscopy of bursa of fabricious of chicks infected with a field strain of infectious bursal disease virus. Acta. Vet. Scand. 29:125–127.
Parton, R. G., and K. Simons. 2007. The multiple faces of caveolae. Nat. Rev. Mol. Cell Biol. 8:185–194.
Pelkmans, L., J. Kartenbeck, and A. Helenius. 2001. Caveolar endocytosis of simian virus 40 reveals a new two-step vesicular-transport pathway to the ER. Nat. Cell Biol. 3:473–483.
Pelkmans, L., and A. Helenius. 2002. Endocytosis via caveolae. Traffic 3:311–320.
PU, L., G. Guay, Y. Altschuler, and I. R. Nabi. 2002. Caveolin-1 is a negative regulator of caveolae-mediated endocytosis to the endoplasmic reticulum. J. Biol. Chem. 277:3371–3379.
Ramm, H. C., T. J. Wilson, R. L. Boyd, H. A. Ward, K. Mitrangas, and K. J. Fahey. 1991. The effect of infectious bursal disease virus on B lymphocytes and bursal stromal components in specific pathogen-free (SPF) White Leghorn chickens. Dev. Comp. Immunol. 15:369–381.
Rautenschlein, S., G. von Samson-Himmelstjerna, and C. Haase. 2007. A comparison of immune responses to infection with virulent infectious bursal disease virus (IBDV) between specific-pathogen-free chickens infected at 12 and 28 days of age. Vet. Immunol. Immunopathol. 115:251–260.
Ravid, D., S. Maor, H. Werner, and M. Liscovitch. 2006. Caveolin-1 inhibits anoikis and promotes survival signaling in cancer cells. Adv. Enzyme Regul. 46:163–175.
Razani, B., and M. Lisanti. 2002. The role of caveolae and the caveolins in mammalian. Physiol. Rev. Under. Res. 1:44–50.
Razani, B., S. E. Woodman, and M. P. Lisanti. 2002. Caveolae: from cell biology to animal physiology. Pharmacol. Rev. 54:431–467.
Rothberg, K. G., J. E. Heuser, W. C. Donzell, Y. S. Ying, J. R. Glenney, and R. G. Anderson. 1992. Caveolin, a protein component of caveolae membrane coats. Cell 68:673–682.
Schoenwolf, G. C., L. A. Bell, and R. L. Watterson. 1981. Vasculogenesis of the bursa cloacalis (bursa of Fabricius) of the chick embryo. J. Morphol. 167:35–42.
Van Deurs, B., K. Roepstorff, A. M. Hommelgaard, and K. Sandvig. 2003. Caveolae: anchored, multifunctional platforms in the lipid ocean. Trends Cell Biol. 13:92–100.
Vervelde, L., and T. F. Davison. 1997. Comparison of the in situ changes in lymphoid cells during infection with infectious bursal disease virus in chickens of different ages. Avian Pathol. 26:803–821.
Warner, G. J., G. Stoudt, M. Bamberger, W. J. Johnson, and G. H. Rothblat. 1995. Cell toxicity induced by inhibition of acyl coenzyme A: cholesterol acyltransferase and accumulation of unesterified cholesterol. J. Biol. Chem. 17:5772–5778.